Biomaterials xxx (2013) 1–10

Contents lists available at SciVerse ScienceDirect

Biomaterials

journal homepage: www.elsevier.com/locate/biomaterials

Fibrous hyaluronic acid hydrogels that direct MSC chondrogenesis through mechanical and adhesive cues

Iris L. Kim [1], Sudhir Khetan [1], Brendon M. Baker [1], Christopher S. Chen [1], Jason A. Burdick*

Department of Bioengineering, University of Pennsylvania, Philadelphia, PA 19104, USA

ARTICLE INFO

Article history:
Received 23 March 2013
Accepted 3 April 2013
Available online xxx

Keywords:
Electrospinning
Mesenchymal stem cells
Hyaluronic acid
Chondrogenesis
Biomaterials
Biomechanics

ABSTRACT

Electrospinning has recently gained much interest due to its ability to form scaffolds that mimic the nanofibrous nature of the extracellular matrix, such as the size and depth-dependent alignment of collagen fibers within hyaline cartilage. While much progress has been made in developing bulk, isotropic hydrogels for tissue engineering and understanding how the microenvironment of such scaffolds affects cell response, these effects have not been extensively studied in a nanofibrous system. Here, we show that the mechanics (through intrafiber crosslink density) and adhesivity (through RGD density) of electrospun hyaluronic acid (HA) fibers significantly affect human mesenchymal stem cell (hMSC) interactions and gene expression. Specifically, hMSC spreading, proliferation, and focal adhesion formation were dependent on RGD density, but not on the range of fiber mechanics investigated. Moreover, traction-mediated fiber displacements generally increased with more adhesive fibers. The expression of chondrogenic markers, unlike trends in cell spreading and cytoskeletal organization, was influenced by both fiber mechanics and adhesivity, in which softer fibers and lower RGD densities generally enhanced chondrogenesis. This work not only reveals concurrent effects of mechanics and adhesivity in a fibrous context, but also highlights fibrous HA hydrogels as a promising scaffold for future cartilage repair strategies.

1. Introduction

Mesenchymal stem cells (MSCs) are commonly used in tissue engineering applications due to their availability, ability to expand, and capacity to differentiate into multiple cell types. It is now widely appreciated that features of the extracellular matrix microenvironment are influential in directing MSC response [1,2]. Two key parameters are matrix mechanics and cellular adhesivity, which have been thoroughly investigated using non-fibrous hydrogels. For example, the elastic modulus of hydrogels presented either as flat, two-dimensional substrates [3,4] or as encapsulating, three-dimensional environments [5] have been shown to dictate stem cell fate. Likewise, the degree of cellular adhesion to the environment (e.g., through changes in ligand density) regulates integrin clustering, cytoskeletal organization, overall morphology, and, specifically in the case of stem cells, differentiation [5–8]. Moreover, RGD density has been shown to influence both chondrogenesis and osteogenesis in alginate hydrogels without significant changes to cell morphology [9,10]. Although studies focusing on either matrix mechanics or integrin binding have demonstrated that each have profound effects on cytoskeletal organization, focal adhesions, and MSC differentiation, the extent to which they act synergistically is less clear [11].

An important clinical application for MSCs under widespread investigation is cartilage repair. Mature hyaline cartilage is avascular and alymphatic, with cells comprising only about 5% of the tissue volume [12]. As a result, trauma or injury to articular cartilage usually leads to progressive tissue degeneration and eventual depletion of healthy cartilage, which can induce pain and discomfort. Current clinical methods to repair defective cartilage are limited in their ability to regenerate functional cartilage both in terms of composition and mechanics [13]. Due to these shortcomings, recent research has focused on the use of tissue engineering approaches to repair cartilage tissue. Particular attention has been given to isotropic, non-fibrous hydrogels as cell carriers due to their high water content and potential for injection into defect sites. MSCs are a common cell source for cartilage tissue engineering strategies, and many groups have tuned hydrogel properties to best support MSC chondrogenesis. Specifically, MSC

* Corresponding author. University of Pennsylvania, Department of Bioengineering, 240 Skirkanich Hall, 210 S. 33rd Street, Philadelphia, PA 19104, USA. Tel.: +1 215 898 8537; fax: +1 215 573 2071.
E-mail address: burdick2@seas.upenn.edu (J.A. Burdick).
[1] Tel.: +215 898 8537; fax: +215 573 2071.

0142-9612/$ – see front matter © 2013 Elsevier Ltd. All rights reserved.
http://dx.doi.org/10.1016/j.biomaterials.2013.04.004

shape and cytoskeletal organization have been shown to significantly regulate chondrogenesis [14,15] and higher RGD densities negatively affected MSC chondrogenesis in a non-fibrous, bulk hydrogel context [10,16]. However, even with significant advances in hydrogel development, these systems lack the depth-dependent, complex mechanical properties of native cartilage [17], motivating the development of additional scaffold approaches.

As an alternative to hydrogels, electrospinning of materials into fibrous scaffolds is gaining interest in cartilage repair due to their ability to mimic the nanofibrous nature of the extracellular matrix, as well as their ability to direct matrix organization [18]. Fibers composed of polycaprolactone (PCL), one of the most commonly used materials in electrospinning systems, have been shown to support not only cell infiltration (with the incorporation of sacrificial fibers or orbital shaking) [19,20], but also MSC chondrogenesis [21–23]. Other electrospun polymers that have been used for chondrogenesis include poly(lactic co-glycolic acid), poly(L-lactic acid), poly(vinyl alcohol), and chitosan [24–27]. Despite the promise of electrospun scaffolds in cartilage repair, the majority of studies examining the effects of fiber properties on MSC chondrogenesis have focused on the effects of fiber diameter [26,28]. Recently, a study with core–shell poly(ether sulfone)-PCL electrospun fibers, in which all material variables were held constant except for mechanics, indicated that lower fiber mechanics increased chondrogenesis of embryonic mesenchymal progenitors [29], further motivating investigation of the influence of fiber parameters on MSC chondrogenesis.

Here, we investigate the chondrogenic differentiation of MSCs on electrospun hyaluronic acid (HA) substrates. HA is an attractive material for cartilage repair applications due to its biological significance; it is involved in many cellular processes including proliferation, morphogenesis, inflammation, and wound repair [30,31]. HA is also important during cartilage development and is differentially regulated during limb bud formation and mesenchymal cell condensation [32]. In direct comparison to PEG hydrogels, HA hydrogels enabled more robust hMSC chondrogenesis and cartilaginous matrix formation both *in vitro* and *in vivo* [33]. Finally, HA is synthetically versatile; methacrylate groups can easily be conjugated to the HA backbone through the hydroxyl groups, and the resulting methacrylated HA (MeHA) is photocrosslinkable [30,34]. Specifically, electrospun MeHA can be crosslinked into cell-adhesive fibers [35,36], and fibrous MeHA scaffolds offer tunable control over mechanics (through the extent of HA modification) and cell adhesivity (through the amount of conjugated RGD). The objective of this work was to understand how variations in these parameters, in the context of a swollen fibrous system, influence hMSC interactions and chondrogenesis.

2. Materials and methods

2.1. Macromer synthesis and scaffold fabrication

MeHA was synthesized as in Ref. [34], with either ~35 or ~100% of the primary hydroxyl groups modified with methacrylates. Briefly, 300 mL of a 1% w/v solution of HA (Lifecore, 64 kDa) was reacted on ice with either 0.67 mL (for 35% modified) or 2.23 mL (for 100% modified) methacrylic anhydride (Sigma) with maintenance of pH at ~7.5–9 for 1.5 days. The products were then dialyzed for 72 h, lyophilized, and the extent of modification was determined with ^{1}H NMR (Bruker). Cysteine-containing RGD peptides (GCGYG*RGDS*PG, Genscript) were conjugated to MeHA via Michael addition between thiols on the peptides and methacrylates on MeHA. For RGD conjugation, MeHA was dissolved at a final concentration of 2% w/v in a pH 8 triethanolamine buffer (Sigma). RGD was added to this solution at varying concentrations (0.3 mM for "low", 1 mM for "medium", or 3 mM for "high"), and the solution was reacted overnight at 37 °C, dialyzed for 48 h, and lyophilized.

MeHA solutions for electrospinning were composed of 4% w/v MeHA, 2% w/v poly(ethylene oxide) (PEO, Sigma, 900 kDa), and 0.5% w/v Irgacure 2959 in deionized water. To electrospin (schematic in Fig. 1A), a syringe was connected to a 12″ long 18G blunt-ended needle positioned 14 cm away from a grounded aluminum mandrel. Using a high voltage power source (Gamma High Voltage Research) and a syringe pump (KD Scientific), the potential difference between the needle and mandrel was adjusted to +21 kV and the solution flow rate was set to a 1.0 mL/h. After collection, electrospun fibers were purged under nitrogen and then crosslinked for 10 min with 10 mW/cm^2 UV light (320–390 nm collimated, Omnicure S1000 UV Spot Cure Systems). Prior to mechanical testing or cell seeding, samples were swollen in PBS at 37 °C for 24–48 h.

2.2. Scaffold imaging and fiber diameter measurements

To measure the diameters of MeHA fibers, samples were electrospun onto foil or methacrylated glass coverslips for dry and swollen measurements, respectively. Glass coverslips were methacrylated as in Ref. [37]. Briefly, 22 × 22 mm coverslips were plasma coated for 3 min to activate the surface, 100 μL of 3-(trimethoxysilyl) propyl methacrylate (Sigma) was applied to the coverslip surface, and the samples were incubated for 1 h at 100 °C followed by 10 min at 110°C. After electrospinning, samples were crosslinked as described and analyzed in both dry and swollen states. Dry fibers were imaged using scanning electron microscopy (SEM, JEOL 7500F HRSEM, Penn Regional Nanotechnology Facility). To visualize swollen fibers under confocal microscopy, a methacrylated rhodamine dye (MeRho, Polysciences) was incorporated prior to electrospinning. Samples were swollen in PBS for 48 h at 37 °C and imaged using confocal microscopy (Zeiss Axioobserver Inverted microscope, Penn CDB Microscopy Core). Fiber diameters (n = 4, 30–40 fibers measured per sample) were measured from the resulting SEM and confocal images for dry and swollen fibers, respectively, using ImageJ (NIH).

2.3. Mechanical testing of single fibers and bulk fibrous hydrogels

In order to measure the moduli of single fibers using atomic force microscopy (AFM), the three-point bending method on single fibers outlined by Tan et al. was adapted [38]. PDMS troughs were fabricated with both a height and trough width of 200 μm (schematic in Fig. 2A) and methacrylated using a modified version of the glass methacrylation protocol described previously. The methacrylated PDMS troughs were then attached to the grounded mandrel parallel to the long axis, and 35% modified and 100% modified MeHA macromers either without RGD or with the highest RGD density (i.e., 3 mM during conjugation) were electrospun onto the troughs. The mandrel was rotating at a speed of 10 m/s during collection to align the fibers perpendicular to the troughs. For fluorescence imaging, MeRho was again incorporated into the solutions prior to electrospinning, and the samples were imaged using a fluorescence microscope. For AFM testing, samples were crosslinked as described before and swollen in a 1% w/v black fabric dye (RIT) solution overnight for visualization under brightfield. Contact-mode AFM (Asylum MFP-3D, University of Pennsylvania Nano/Bio Interface Center) was then performed using a 25 μm, silicon bead AFM tip with a spring constant of 0.06 N/m (Novascan). Only single fibers perpendicular to the direction of the troughs were measured, as differences in fiber angle or testing multiple fibers at once would confound the measurements. Images were taken of each trough to measure the distance between trough edges, and the average fiber diameter was used to calculate the modulus of each fiber. A total of 10–12 fibers per condition were measured. The force and displacement (δ) measurements were then used to calculate the modulus of the fibers based on the equations used in Tan et al. [38].

For mechanical testing of bulk, fibrous hydrogels, both 35% modified and 100% modified MeHA were electrospun for 4 h. After crosslinking, fibrous mats were trimmed to create samples 4 mm in diameter, and samples were swollen in PBS at 37 °C for 24 h prior to testing. Unconfined compression testing was performed on swollen samples using a dynamic mechanical analyzer (Q800 TA Instruments) at a strain rate of 10%/min, and moduli were calculated at a strain from 10% to 20% (n = 4–6).

2.4. Cell seeding and assessment of spreading, proliferation, and focal adhesion formation

For *in vitro* studies, fibers were collected onto methacrylated glass coverslips, crosslinked, and swollen as described above. Both 35% and 100% modified MeHA macromers were electrospun with varying amounts of RGD (0.3, 1, and 3 mM during peptide conjugation). hMSCs were seeded onto the fibrous scaffolds in growth media (α-MEM with 20% FBS, 1% L-glutamine, and 1× penicillin/streptomycin) by direct addition of the cell suspension onto the fibrous sample and subsequent overnight incubation. For assessment of cell spreading, proliferation, and focal adhesion formation, hMSCs were seeded onto the scaffolds at a density of 15, 20, or 25 thousand cells per cm^2 corresponding to the high (3 mM), medium (1 mM), and low (0.3 mM) RGD density groups, respectively. The varied cell densities were used based on differential initial cell adhesion, to obtain comparable initial cell numbers between groups. After overnight incubation, cell-seeded scaffolds were cultured in chemically-defined chondrogenic differentiation media (CM+) consisting of high glucose DMEM with 1× penicillin/streptomycin, 0.1 mM dexamethasone, 50 mg/ml ascorbate 2-phosphate, 40 mg/ml L-proline, 100 mg/ml sodium pyruvate, 1× ITS+ (6.25 mg/ml insulin, 6.25 mg/ml transferrin, 6.25 ng/ml selenous acid, 1.25 mg/ml bovine serum albumin, and 5.35 mg/ml linoleic acid), and 10 ng/mL TGF-β3 (R&D

Please cite this article in press as: Kim IL, et al., Fibrous hyaluronic acid hydrogels that direct MSC chondrogenesis through mechanical and adhesive cues, Biomaterials (2013), http://dx.doi.org/10.1016/j.biomaterials.2013.04.004

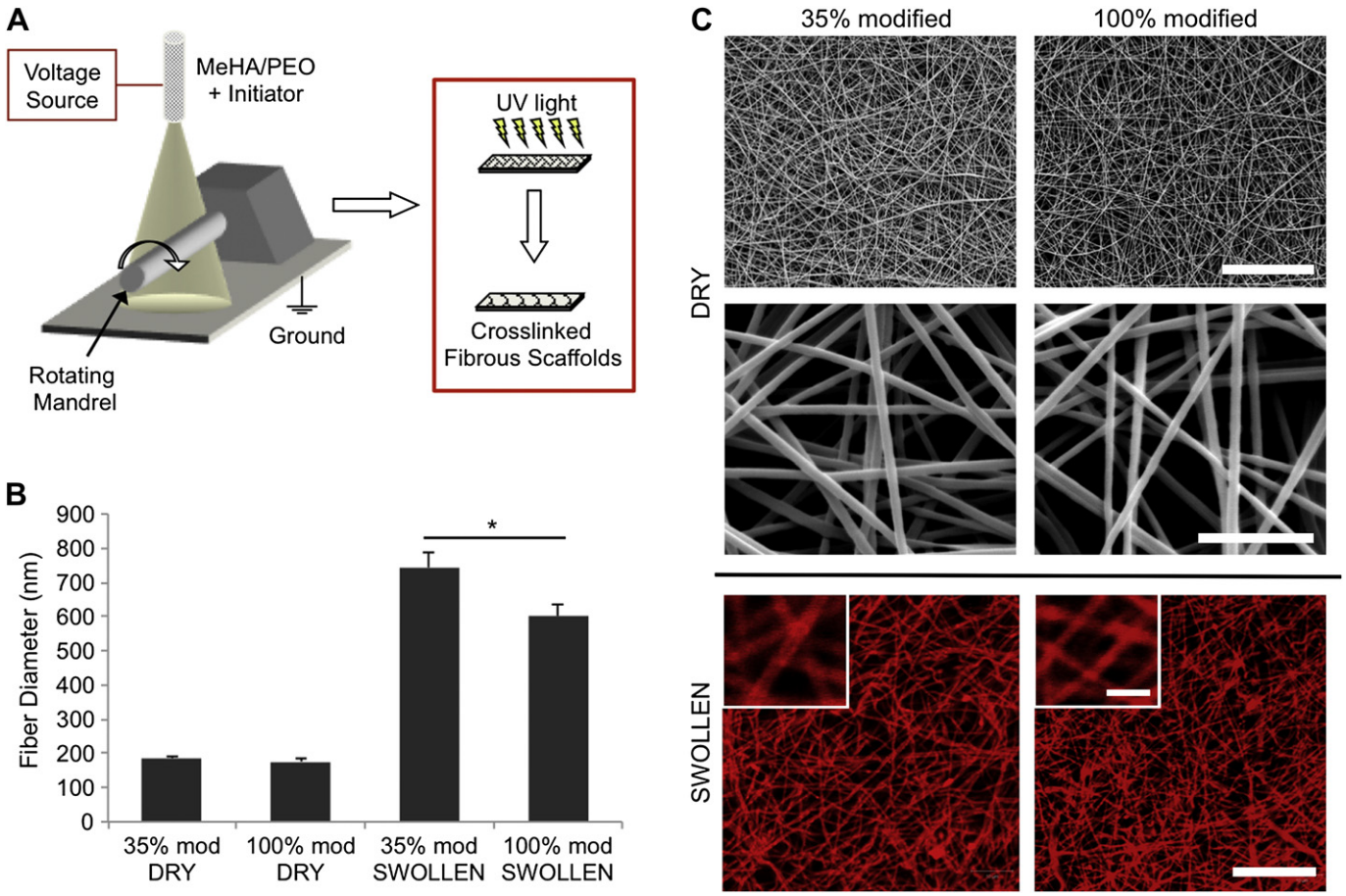

Fig. 1. (A) Schematic of electrospinning system. Hyaluronic acid macromer fibers (containing photoinitiator) are crosslinked with UV light after electrospinning. (B) Diameters of dry and swollen MeHA fibers ($n = 30–40$) fabricated from either 35% or 100% modified MeHA. (C) Representative SEM images of dry MeHA fibers (top and middle rows) and confocal images of swollen MeHA fibers (bottom row, with methacrylated rhodamine for visualization). Scale bars: 10 μm for top row, 2 μm for middle row, 20 μm for bottom row, and 5 μm for inset of bottom row.

Systems). After 1, 7, and 14 days of culture, samples were fixed in 4% phosphate-buffered formalin and stained for actin cytoskeleton (phalloidin), nuclei (DAPI), and vinculin (primary monoclonal mouse anti-human vinculin, Sigma, and secondary FITC-conjugated goat anti-mouse, Invitrogen) ($n = 4$). Cell areas and proliferation were determined (>100 cells per condition) with ImageJ using the actin and DAPI staining, respectively.

2.5. Chondrogenic gene expression

For gene expression studies, fibers were collected onto methacrylated PDMS (to allow for samples with larger areas, and subsequently, a greater number of cells per sample). hMSCs were seeded onto these fibrous scaffolds at the same cell densities stated above and cultured in CM+. After 14 days of culture, the samples were rinsed with PBS and scraped off the underlying PDMS into 1.5 mL Eppendorf tubes containing Trizol reagent (Invitrogen). The samples were manually homogenized, and RNA was extracted using manufacturer's instructions. RNA concentration was determined using an ND-1000 spectrophotometer (Nanodrop Technologies). After 1 μg of RNA from each sample was reverse transcribed, PCR was performed on an Applied Biosystems 7300 Real-Time PCR system ($n = 4$). Relative gene expression for Type I collagen, Type II collagen, aggrecan, and sox-9 was calculated using the $\Delta\Delta C_T$ method with GAPDH as a housekeeping gene. Sequences used for primers and probes can be found in Ref. [39].

2.6. Analysis of cell-induced bead displacements

For bead displacement studies, fluorescent polystyrene beads (Suncoast Yellow and Yellow Green, Bangs Laboratories) were incorporated into the macromer solutions prior to electrospinning. Samples were electrospun onto methacrylated circular coverslips. After crosslinking and swelling of the samples overnight, hMSCs were seeded at a density of 1000, 2000, or 4000 cells/cm^2 corresponding to the high, medium, and low RGD density groups, respectively, as described above. Bead displacements were measured after 24 h using an adaptation of the method described by Legant et al. [40]. Briefly, after overnight culture in growth media, cells were stained with calcein AM (Invitrogen), and the samples were transferred to an Attofluor® Cell Chamber (Invitrogen) and maintained at 37 °C and 5% CO_2 during imaging. Confocal microscopy was used to obtain z-stacks of the cells and surrounding fluorescent beads before and after cell lysis, induced by the addition of 5% w/v SDS. Samples were allowed to equilibrate after SDS addition for 20–30 min prior to imaging. Tecplot, Hypermesh, and MATLAB were then used to quantify bead displacements from resulting z-stacks. Bead displacements were sorted by distance from the cell boundary, and the displacements of beads 15 μm or closer to the cell were included in the average ($n = 10–12$).

2.7. Statistical analysis

For comparison of two groups, a student's t-test with a p-value of 0.05 was used to measure statistical significance. For analyses with more than one comparison, a one-way ANOVA was performed followed by a Bonferroni post hoc test. For graphs and text, values are reported as mean ± standard error.

3. Results

3.1. MeHA fibrous scaffold fabrication and characterization

Both 35% and 100% modified MeHA macromers were synthesized, conjugated with RGD, electrospun, and crosslinked successfully into fibrous scaffolds (Fig. 1). Fiber morphology was consistent throughout all studies, with no apparent beading or spraying observed in SEM or confocal images. Fiber diameters of dry fibers were 186 ± 7 nm for 35% modified MeHA and 177 ± 6 nm for 100% modified MeHA, with a notable increase in fiber diameter upon

Please cite this article in press as: Kim IL, et al., Fibrous hyaluronic acid hydrogels that direct MSC chondrogenesis through mechanical and adhesive cues, Biomaterials (2013), http://dx.doi.org/10.1016/j.biomaterials.2013.04.004

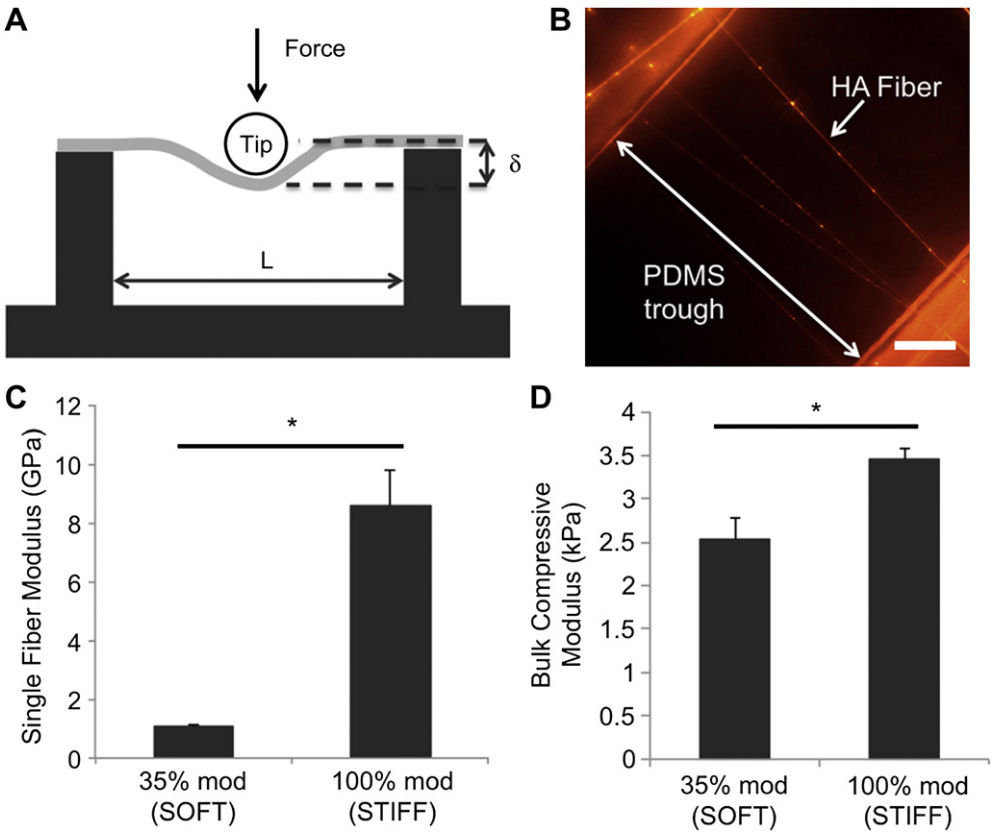

Fig. 2. (A) Schematic of contact-mode AFM on single fibers suspended over PDMS troughs. Image is not to scale. (B) Fluorescence image of swollen HA fibers (with methacrylated rhodamine for visualization) suspended over a PDMS trough. Scale bar = 50 μm. (C) Three-point bending moduli of soft and stiff single fibers ($n = 10–12$). (D) Compressive moduli of bulk, fibrous hydrogels composed of soft or stiff fibers ($n = 4–6$). * denotes statistical significance ($p < 0.05$).

swelling to 601 ± 36 and 744 ± 45 nm for 100% and 35% modified MeHA, respectively (Fig. 1B). The fiber diameters of swollen scaffolds were constant and did not change over 14 days incubation in PBS (data not shown), indicating that nearly all swelling occurred during the first 24 h. Based on initial sample weight and volumetric swelling ratios (data not shown) and assuming a homogeneous network, the overall RGD densities within the swollen, fibrous scaffolds were estimated to be 0.27 mM, 0.90 mM, and 2.7 mM for the "low", "medium", and "high" RGD groups. These estimates are based on the overall scaffold volume (i.e., including the void spaces between fibers), although RGD is localized to the fibers.

To mechanically characterize the MeHA fibers, both 35% modified and 100% modified MeHA solutions were electrospun onto PDMS troughs and clearly visualized with fluorescence microscopy, as shown in Fig. 2B. The average trough length was much greater than the diameter of the bead tip, fulfilling a necessary condition for the validity of the model [38]. Most fibers were perpendicular to the PDMS troughs, which was achieved through the high rotating speed of the grounded mandrel. The resulting bending moduli for fibers without RGD were 1.06 ± 0.06 and 8.60 ± 1.18 GPa for 35% modified and 100% modified MeHA fibers, respectively (Fig. 2C). For single fibers of the same % modification, there were no significant differences in bending moduli between fibers without RGD and fibers with the highest RGD density (1.17 ± 0.29 and 7.29 ± 1.11 GPa for 35% modified and 100% modified MeHA, respectively). Bulk compressive moduli were generally much lower than bending moduli of single fibers, with values of 2.53 ± 0.25 kPa for 35% modified fibrous samples and 3.46 ± 0.12 kPa for 100% modified fibrous samples (Fig. 2D). The differences in both single fiber bending moduli and bulk compressive moduli were statistically significant between 35% modified and 100% modified MeHA fibers, and here forward, the 35% and 100% modified MeHA conditions are referred to as 'soft' and 'stiff', respectively.

3.2. hMSC adhesion, spreading, and proliferation on fibers

When hMSCs were seeded onto fibrous MeHA scaffolds of varying fiber mechanics and RGD densities, initial adhesion (i.e., the number of cells that were adhered 24 h after seeding) was dependent on both the cell seeding density and RGD density (data not shown). With the same cell seeding density of 15×10^3 cells/cm^2, the initial number of cells adhering after 24 h increased with RGD density (e.g., 6.55×10^3 cells/cm^2, 8.82×10^3 cells/cm^2, and 11.8×10^3 cells/cm^2, for low, medium, and high RGD modified soft fibers, respectively). For this reason, cell seeding densities were modified to account for differences in initial adhesion in order to begin all *in vitro* studies (with the exception of fiber displacement studies) with a similar cell density across all groups. Over 14 days of culture in CM+, hMSCs increased in spread area on higher RGD density scaffolds (Fig. 3). Histograms of cell area (quantified after 24 h of culture) were normalized to the total number of measurements per condition and reported as a % of total cells (Fig. 4A). As observed in the actin-stained images, the average cell area increased with increasing RGD density for both fiber moduli. hMSCs seeded on scaffolds with low RGD density were uniformly less spread, whereas hMSCs on the high RGD groups exhibited greater average spread areas, as well as greater variance in spreading. There were no significant differences in cell spreading between hMSCs on soft and on stiff fibers when presented the same

Please cite this article in press as: Kim IL, et al., Fibrous hyaluronic acid hydrogels that direct MSC chondrogenesis through mechanical and adhesive cues, Biomaterials (2013), http://dx.doi.org/10.1016/j.biomaterials.2013.04.004

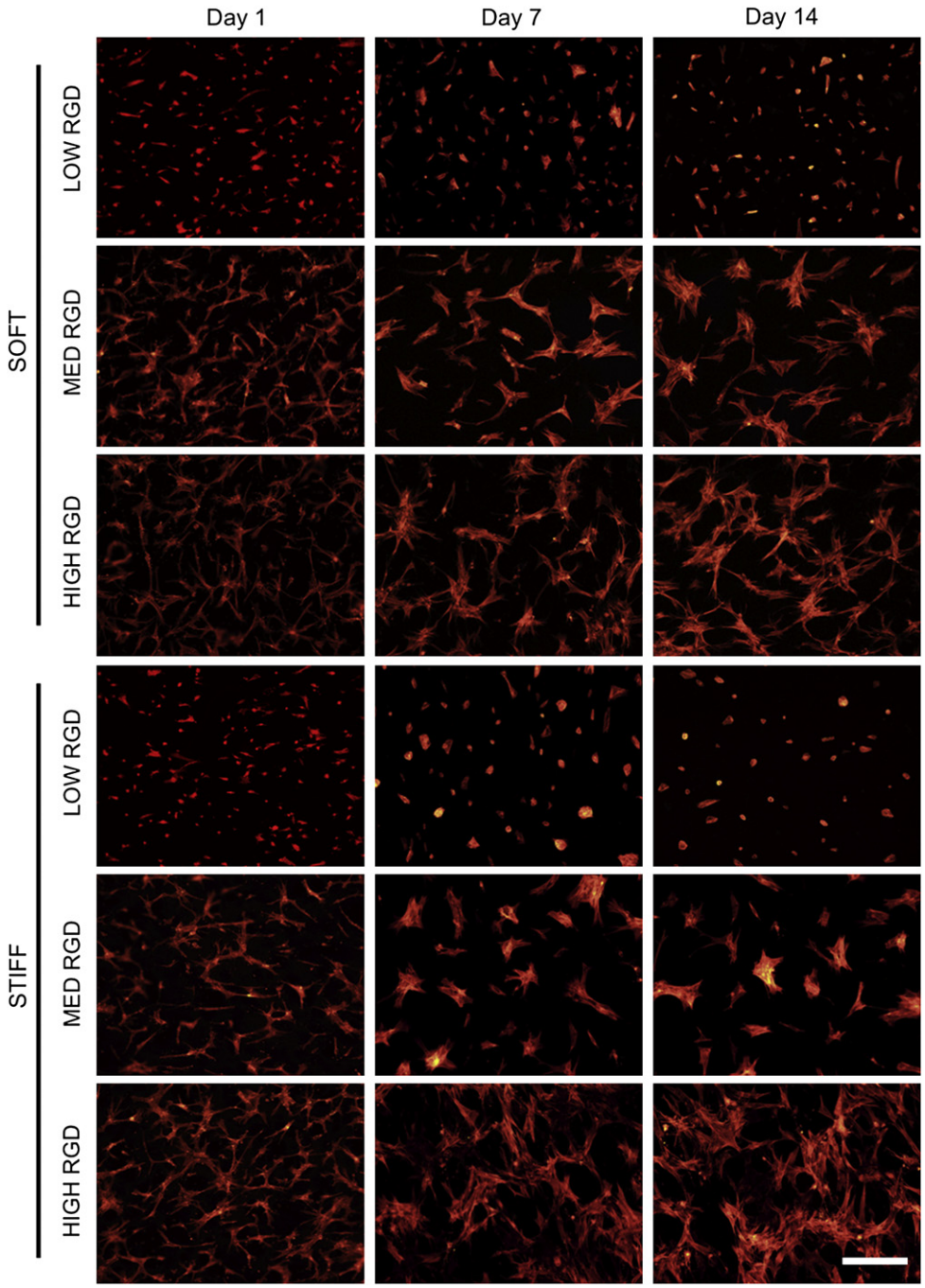

Fig. 3. hMSCs cultured in CM+ and stained with TRITC-phalloidin after 1, 7, and 14 days of *in vitro* culture. Scale bar: 400 μm.

RGD density. Multicellular aggregates were more apparent with longer incubation times and higher RGD densities.

Proliferation was determined by quantifying the density of cell nuclei at each time point relative to day one values for each group. Thus, a value less than 1 signifies a decrease in cell density with time, whereas a value greater than 1 signifies an increase in cell density with time. Proliferation was dependent on RGD density; the cell populations corresponding to the two higher RGD densities exhibited significant increases in proliferation relative to the lowest RGD density (Fig. 4B). However, hMSC proliferation was relatively similar when the fiber mechanics were changed, with the exception of a significant increase due to modulus at the highest RGD density after 7 days of culture. Nonetheless, it is important to note that proliferation was overall limited, as no groups reached a normalized proliferation index of 2 (i.e., cell doubling) after 14 days of culture even with the highest amount of RGD. Vinculin organization after 24 h followed expected trends based on cell spreading, with more numerous vinculin-rich adhesions near the cell periphery of well-spread cells (higher RGD densities) and more diffuse organization in rounded cells (lower RGD densities) (Fig. 5). There were no discernible differences in vinculin organization between groups with different mechanics and the same RGD density and this trend persisted throughout the 14 days of culture in CM+ (data not shown).

Please cite this article in press as: Kim IL, et al., Fibrous hyaluronic acid hydrogels that direct MSC chondrogenesis through mechanical and adhesive cues, Biomaterials (2013), http://dx.doi.org/10.1016/j.biomaterials.2013.04.004

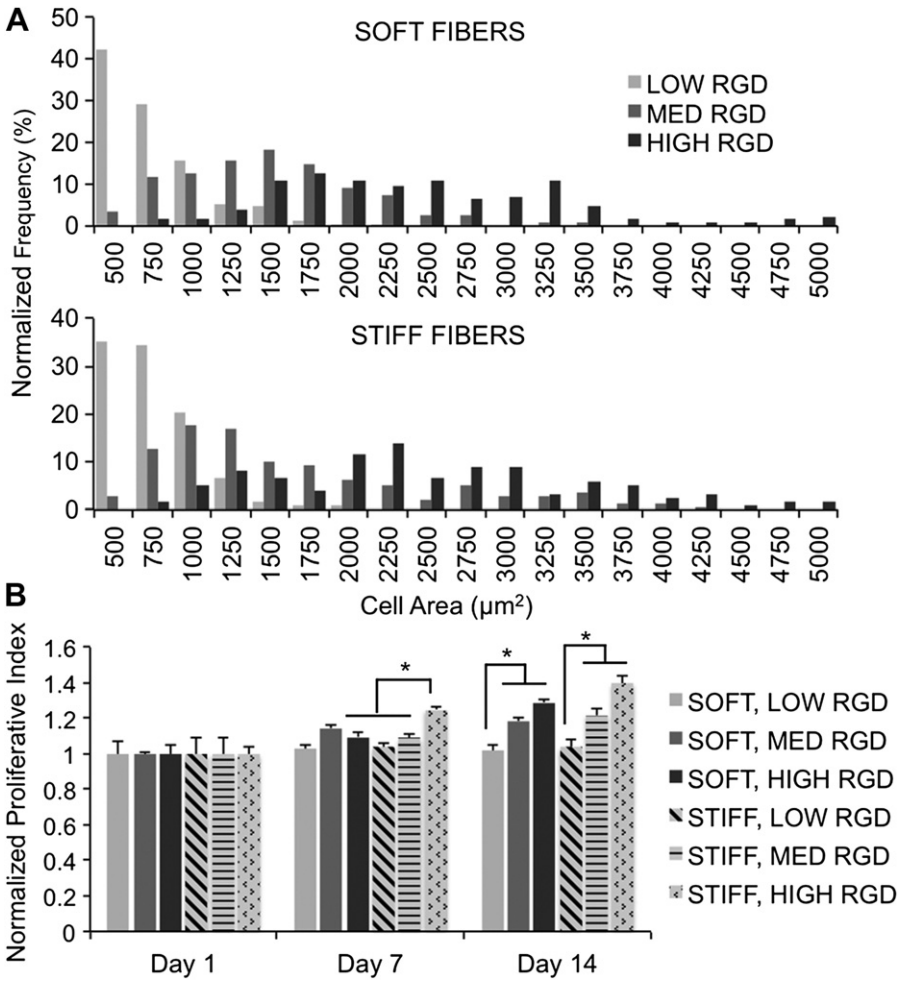

Fig. 4. (A) hMSC cell spread area after 24 h, quantified with TRITC-phalloidin staining and reported as normalized frequency (%) ($n = 100–120$). (B) hMSC proliferation, as measured by quantification of nuclei, for 1, 7, or 14 days of culture in CM+ ($n = 4$), with changes in fiber RGD density and modulus. Normalized proliferative index calculated as nuclei density at the specified time point normalized to the average nuclei density after one day of culture. * denotes statistical significance ($p < 0.05$).

3.3. hMSC chondrogenesis

In contrast to hMSC spreading, proliferation, and focal adhesion formation, which were all unaffected by changes in the fiber mechanics investigated, hMSC gene expression after 14 days of culture in CM+ was dependent on both fiber mechanics and RGD density (Fig. 6). Type II collagen, aggrecan, and sox-9 are markers for chondrogenic differentiation, whereas Type I collagen indicates transformation to a more fibrotic phenotype. Gene expression profiles were determined using the $\Delta\Delta C_T$ method normalized to GAPDH expression. RGD density had a profound effect on hMSC gene expression profiles. For instance, the lowest RGD density, soft fiber group resulted in a 405k-, 6.66-, and 3.58-fold increase in gene expression of Type II collagen, aggrecan, and sox-9, respectively, whereas the highest RGD, soft fiber group resulted in a 233-fold increase in Type II collagen and a decrease in both aggrecan and sox-9 (values of 0.94 and 0.23, respectively). Although the dependence of hMSC gene expression on fiber mechanics was not as pronounced as that of RGD density, chondrogenic gene expression was consistently higher with soft fibers when compared to stiff fibers, and this difference was statistically significant for aggrecan at the lowest RGD density. Additionally, Type I collagen was consistently up-regulated with stiff fibers when compared to soft fibers, although the differences were not statistically significant.

3.4. hMSC-induced bead displacements

An indirect method to evaluate cell-mediated traction forces was used to assess whether hMSCs displaced fibers. Average bead displacements were calculated based on confocal *z*-stacks of fluorescent beads before and after cell lysis; bead displacements can serve as a proxy for traction forces across different RGD densities as long as fiber mechanics are held constant. Contraction-mediated bead displacements, and thus presumably traction forces, generally increased with RGD density, though this trend was more pronounced for the soft fiber condition compared to the stiff fiber condition (Fig. 7A). Most of the average bead displacements were relatively small (<0.5 μm), but those corresponding to the high RGD density, soft fiber condition exhibited a significantly greater average bead displacement (1.2 μm) relative to the low and medium RGD densities, soft fiber conditions (Fig. 7B). Stiff fibers generally resulted in lower bead displacements in comparison to soft fibers, but no conclusions can be drawn on differences in cell traction forces between soft and stiff fibers.

4. Discussion

Matrix mechanics and adhesivity (i.e., incorporation of ligands for integrin binding) have been studied extensively in non-fibrous

Please cite this article in press as: Kim IL, et al., Fibrous hyaluronic acid hydrogels that direct MSC chondrogenesis through mechanical and adhesive cues, Biomaterials (2013), http://dx.doi.org/10.1016/j.biomaterials.2013.04.004

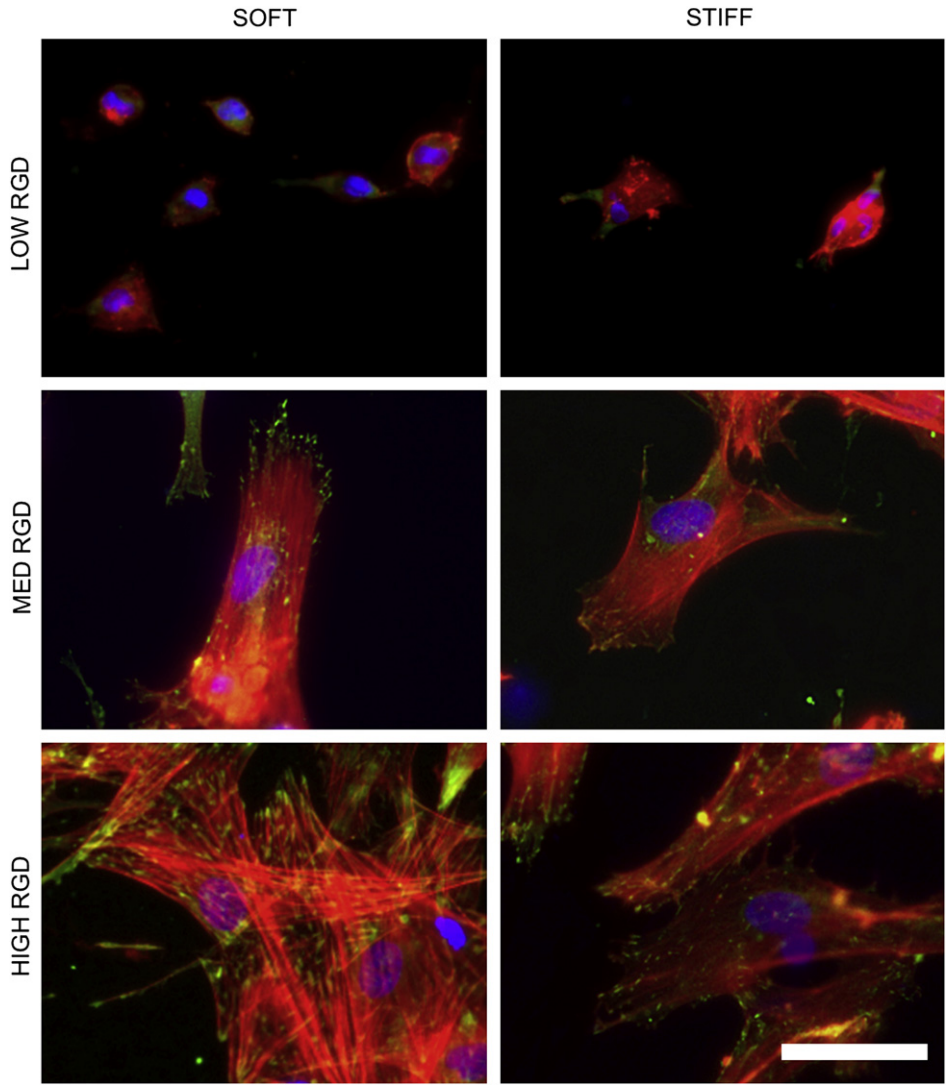

Fig. 5. Vinculin localization (green), actin cytoskeleton (red), and nuclei (blue) staining for hMSCs cultured for 24 h on fibrous scaffolds with varied RGD density and modulus. Scale bar: 50 μm. (For interpretation of the references to colour in this figure legend, the reader is referred to the web version of this article.)

settings, primarily via seeding of cells atop flat, two-dimensional substrates. In the case of cartilage, both of these variables have been shown to affect chondrocyte redifferentiation in a non-fibrous, three-dimensional context [41]. Specifically, chondrocytes that had dedifferentiated during expansion on TCPS exhibited enhanced redifferentiation when encapsulated within bulk hydrogels of lower RGD densities and lower equilibrium moduli. Moreover, the presence of RGD has been shown to negatively affect chondrogenesis of MSCs in bulk hydrogels [10,16]. In contrast to these non-fibrous hydrogel systems, cartilage possesses a fibrillar structure with depth-dependent anisotropy, and thus fibrous scaffolds may be a more appropriate setting to investigate the effects of the microenvironment on MSC chondrogenesis. For these reasons, fibrous HA scaffolds were developed here as a system to investigate the effects of both mechanics and RGD density on MSC response, since we can controllably tune both parameters within fibers composed of a biologically relevant material.

Due to the high viscosity and surface tension of HA solutions, electrospinning of HA alone typically requires harsh solvents or complicated electro-blowing systems [42–44]. PEO was thus used as a carrier polymer to successfully and stably electrospin HA into fibrous scaffolds. Since HA is hydrophilic and was electrospun at a low molecular weight, it was necessary to crosslink prior to swelling to retain the fibrous nature. Crosslinking was achieved through a photoinitiated radical polymerization of methacrylates along the macromer backbone. The final crosslinking density was controlled through HA modification (35% versus 100%), corresponding to nearly an order of magnitude difference in post-swelling single fiber bending moduli (1 GPa versus 8.6 GPa, respectively). Both the “soft” and “stiff” fiber populations swelled significantly (on average, the fiber diameters increased 3- and 4-fold relative to the dry state for 100% modified and 35% modified MeHA fibers, respectively). The moduli of both fiber conditions, while relatively high (in the GPa range), are comparable to values reported for single fibers of electrospun collagen, PLGA, and PCL [38,45–48]. The relatively high moduli may also be a result of the densely crosslinked nature of the HA macromer chains, since the fibers are crosslinked while dry. Furthermore, the moduli of both fibrous systems dropped significantly when measured in bulk instead of on the single fiber level, most likely due to the large amount of void space within the scaffold.

To ensure a similar initial cell density (i.e., the density of cells that adhered to the scaffold during overnight incubation) between groups, various cell seeding densities (i.e., the number of cells

Please cite this article in press as: Kim IL, et al., Fibrous hyaluronic acid hydrogels that direct MSC chondrogenesis through mechanical and adhesive cues, Biomaterials (2013), http://dx.doi.org/10.1016/j.biomaterials.2013.04.004

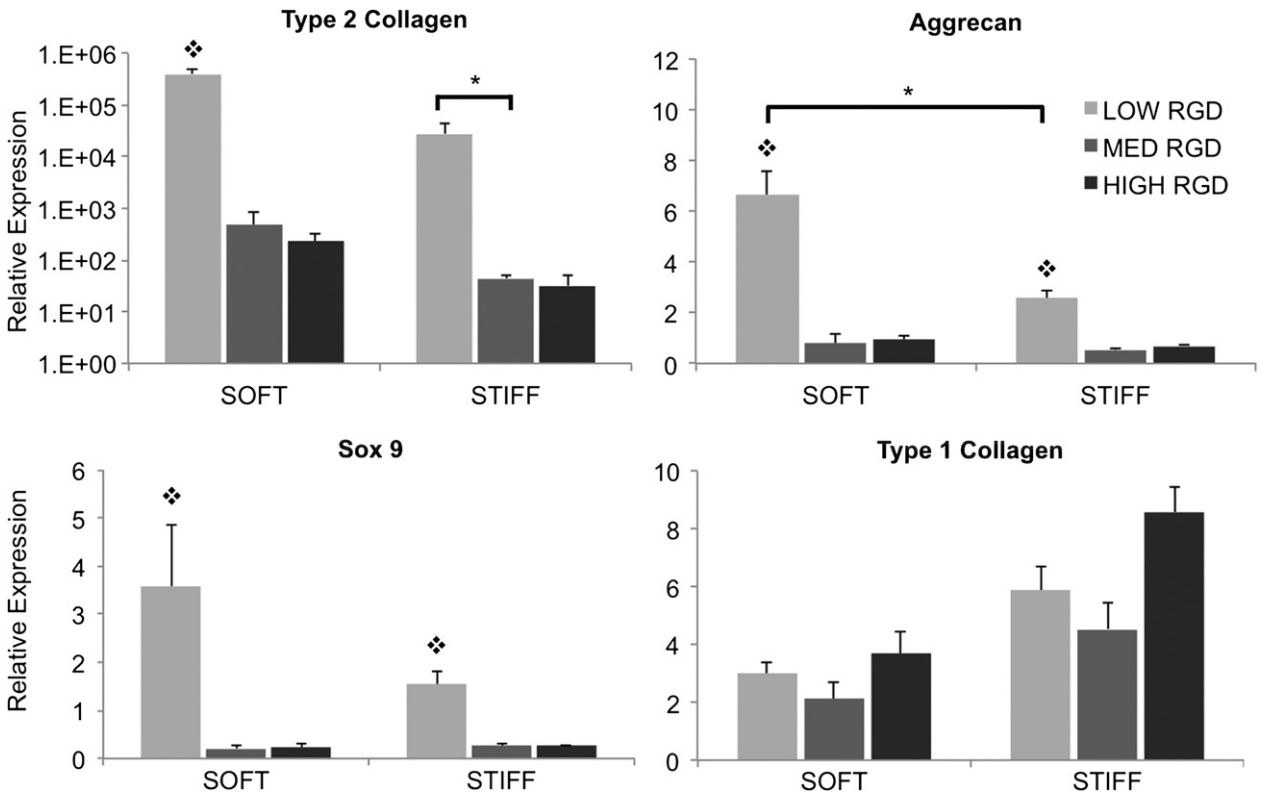

Fig. 6. hMSC gene expression of chondrogenic markers after 14 days of culture in CM + on fibrous scaffolds with varied RGD density and modulus. * denotes statistical significance ($p < 0.05$) between indicated groups, and ❖ denotes statistical significance ($p < 0.05$) when compared to other RGD densities within the same fiber stiffness condition.

added to each well) were tested. The initial cell density was dependent on both the number of cells added to the scaffold-containing well and the RGD density; thus, hMSCs were seeded onto fibrous HA scaffolds at increasing initial cell densities for decreasing RGD densities. Throughout the 2 weeks of culture in CM+, hMSCs responded to RGD density but were insensitive to the range of fiber mechanics investigated in terms of cell spreading, proliferation, cytoskeletal organization, and focal adhesion formation (Figs. 3–5). The apparent lack of hMSC response (other than in gene expression profiles) between the two fiber mechanics groups

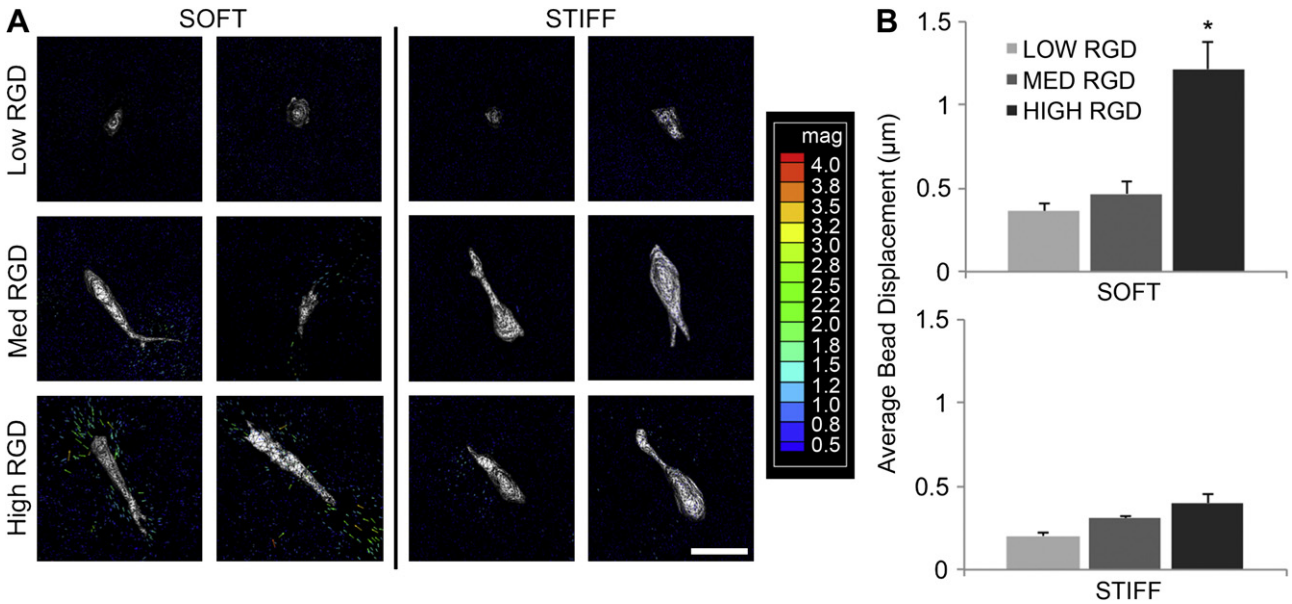

Fig. 7. (A) hMSC bead displacements after 24 h of culture on fibrous scaffolds with varied RGD density and modulus ($n = 10–12$). Color-coded scale bar is for bead displacements and in units of μm. Scale bar: 40 μm. (B) Average bead displacement values for beads within 15 μm of the cell boundary for hMSCs cultured on either soft or stiff fibrous scaffolds with varied RGD density. * denotes statistical significance ($p < 0.05$) when compared to all other conditions.

Please cite this article in press as: Kim IL, et al., Fibrous hyaluronic acid hydrogels that direct MSC chondrogenesis through mechanical and adhesive cues, Biomaterials (2013), http://dx.doi.org/10.1016/j.biomaterials.2013.04.004

may be due to the fibrous topography. Topography can have significant effects on hMSC response; fibrous PCL scaffolds were shown to enhance hMSC chondrogenesis in comparison to porous PCL scaffolds [23], and nanoscale grooves and ridges have been shown to affect hMSC spreading and differentiation [49–51]. The fibrous architecture, in comparison to flat 2-dimensional surfaces [3], may increase the ability of cells to spread and pull, even with softer matrices.

Chondrogenesis is typically characterized by up-regulation of Type II collagen, aggrecan, and sox-9 and down-regulation of Type I collagen. Despite similarities in adhesion, spreading, and proliferation, the gene expression analysis presented here suggests that cells sense the difference in fiber mechanics, as the soft fiber condition generally promoted a greater degree of chondrogenesis. RGD density was a critical regulator of this lineage commitment, since statistically significant increases for all pro-chondrogenic genes were observed only at lower RGD densities. Type I collagen was more highly expressed with the stiffer fibers and higher RGD density conditions. These findings correlate well with previous studies performed with non-fibrous bulk hydrogels, with lower elastic moduli and lower RGD densities resulting in either improved hMSC chondrogenesis or chondrocyte redifferentiation [10,41].

Traction forces are another important indicator of how cells interact with their surrounding matrix. Cell-mediated traction forces correlate directly with cytoskeletal tension, which has been shown to regulate cellular functions ranging from proliferation to differentiation [52,53]. A modified method from Ref. [54] was implemented to measure bead displacements and to obtain a relative measure of cell-mediated traction forces. For cells interacting with fibrous scaffolds, absolute traction forces are difficult to calculate since fibrous scaffolds are heterogeneous and non-uniform networks, complicating the correlation of bead displacement and force used in the aforementioned method. However, within a group of fibers of the same modulus, differences in bead displacements can be correlated with differences in traction forces. hMSCs interacting with MeHA fibers caused greater average bead displacements, and thus presumably traction forces, with increasing RGD densities. These differences were statistically significant for the soft fiber condition but not the stiff fiber condition, although the trend was still apparent in the latter case. Similarities in cell spreading and focal adhesion formation between the conditions suggest that cells on stiff fibers are exerting traction forces to some extent, but that the bead displacements are lower since the fiber moduli are greater.

Finally, the fibrous system developed here focuses on cell studies using hMSCs seeded on top of the material. Although this does constitute a quasi-3D system, as cells can extend into the underlying fibrous network, the cells are not completed embedded within a fibrous matrix, which may better mimic the natural presentation of the extracellular matrix *in vivo*. Additionally, the range of fiber mechanics studied may not have been great enough to influence changes in cell behavior in many of the metrics used in this work. Despite these limitations, this study presents a system with which to probe MSC interactions with fibrous materials.

5. Conclusions

This work demonstrates the processing of HA into fibrous hydrogels with tunable mechanics and adhesivity using an electrospinning process. Adhesivity had a strong influence on hMSC response, with higher RGD densities leading to increases in cell spreading, proliferation, and focal adhesion formation. Both parameters were found to influence hMSC chondrogenesis, as seen through gene expression profiles, potentially by differentially enabling cytoskeletal organization and the resulting ability of cells to exert tractions on the fibers. Given these findings, we believe that fibrous HA hydrogels are a promising alternative to non-fibrous hydrogels as a platform to study MSC chondrogenesis and for future cartilage regeneration strategies.

Acknowledgements

This work was supported by National Institutes of Health grants R01EB008722 and R01GM74048, National Science Foundation Major Research Instrumentation Grant DBI-0721913, National Science Foundation Nanoscale Science and Engineering Center grant DMR-0425780, and a National Science Foundation Graduate Research Fellowship to ILK. BMB acknowledges support from a Ruth L. Kirschtein National Research Service Award F32EB014691.

References

[1] Marklein RA, Burdick JA. Controlling stem cell fate with material design. Adv Mater 2010;22:175–89.
[2] Wade RJ, Burdick JA. Engineering ECM signals into biomaterials. Mater Today 2012;15:454–9.
[3] Engler A, Sen S, Sweeney H, Discher D. Matrix elasticity directs stem cell lineage specification. Cell 2006;126:677–89.
[4] Guvendiren M, Burdick JA. Stiffening hydrogels to probe short- and long-term cellular responses to dynamic mechanics. Nat Commun 2012;3:792.
[5] Huebsch N, Arany PR, Mao AS, Shvartsman D, Ali OA, Bencherif SA, et al. Harnessing traction-mediated manipulation of the cell/matrix interface to control stem-cell fate. Nat Mater 2010;9:518–26.
[6] Cukierman E, Pankov R, Stevens DR, Yamada KM. Taking cell-matrix adhesions to the third dimension. Science 2001;294:1708–12.
[7] Kato M, Mrksich M. Using model substrates to study the dependence of focal adhesion formation on the affinity of integrin–ligand complexes. Biochemistry 2004;43:2699–707.
[8] Wang X, Yan C, Ye K, He Y, Li Z, Ding J. Effect of RGD nanospacing on differentiation of stem cells. Biomaterials 2013;34:2865–74.
[9] Comisar WA, Kazmers NH, Mooney DJ, Linderman J. Engineering RGD nanopatterned hydrogels to control preosteoblast behavior: a combined computational and experimental approach. Biomaterials 2007;28:4409–17.
[10] Connelly JT, García AJ, Levenston ME. Inhibition of in vitro chondrogenesis in RGD-modified three-dimensional alginate gels. Biomaterials 2007;28:1071–83.
[11] Rowlands AS, George PA, Cooper-White JJ. Directing osteogenic and myogenic differentiation of MSCs: interplay of stiffness and adhesive ligand presentation. Am J Physiol Cell Physiol 2008;295:C1037–44.
[12] Chung C, Burdick J. Engineering cartilage tissue. Adv Drug Deliv Rev 2008;60:243–62.
[13] Ahmed TAE, Hincke MT. Strategies for articular cartilage lesion repair and functional restoration. Tissue Eng Part B Rev 2010;16:305–29.
[14] Gao L, McBeath R, Chen CS. Stem cell shape regulates a chondrogenic versus myogenic fate through Rac1 and N-cadherin. Stem Cells 2010;28:564–72.
[15] Woods A, Beier F. RhoA/ROCK signaling regulates chondrogenesis in a context-dependent manner. J Biol Chem 2006;281:13134–40.
[16] Salinas C, Anseth K. The influence of the RGD peptide motif and its contextual presentation in PEG gels on human mesenchymal stem cell viability. J Tissue Eng Regen Med 2008;2:296–304.
[17] Huang AH, Farrell MJ, Mauck RL. Mechanics and mechanobiology of mesenchymal stem cell-based engineered cartilage. J Biomech 2010;43:128–36.
[18] Baker BM, Handorf AM, Ionescu LC, Li W-J, Mauck RL. New directions in nanofibrous scaffolds for soft tissue engineering and regeneration. Expert Rev Med Devices 2009;6:515–32.
[19] Baker BM, Gee AO, Metter RB, Nathan AS, Marklein RA, Burdick JA, et al. The potential to improve cell infiltration in composite fiber-aligned electrospun scaffolds by the selective removal of sacrificial fibers. Biomaterials 2008;29:2348–58.
[20] Nerurkar NL, Sen S, Baker BM, Elliott DM, Mauck RL. Dynamic culture enhances stem cell infiltration and modulates extracellular matrix production on aligned electrospun nanofibrous scaffolds. Acta Biomater 2011;7:485–91.
[21] Alves da Silva ML, Martins A, Costa-Pinto AR, Costa P, Faria S, Gomes M, et al. Cartilage tissue engineering using electrospun PCL nanofiber meshes and MSCs. Biomacromolecules 2010;11:3228–36.
[22] Li W-J, Tuli R, Okafor C, Derfoul A, Danielson KG, Hall DJ, et al. A three-dimensional nanofibrous scaffold for cartilage tissue engineering using human mesenchymal stem cells. Biomaterials 2005;26:599–609.
[23] Wise JK, Yarin AL, Megaridis CM, Cho M. Chondrogenic differentiation of human mesenchymal stem cells on oriented nanofibrous scaffolds: engineering the superifical zone of articular cartilage. Tissue Eng Part A 2009;15:913–21.

Please cite this article in press as: Kim IL, et al., Fibrous hyaluronic acid hydrogels that direct MSC chondrogenesis through mechanical and adhesive cues, Biomaterials (2013), http://dx.doi.org/10.1016/j.biomaterials.2013.04.004

[24] Spaddacio C, Rainer A, Trombetta M, Vadala G, Chello M, Covino E, et al. Poly-L-lactic acid/hydroxyapatite electrospun nanocomposites induce chondrogenic differentiation of human MSC. Ann Biomed Eng 2009;37:1376–89.
[25] Xin X, Hussain M, Mao J. Continuing differentiation of human mesenchymal stem cells and induced chondrogenic and osteogenic lineages in electrospun PLGA nanofiber scaffold. Biomaterials 2007;28:316–25.
[26] Noriega S, Hasanova G, Schneider M, Larsen G, Subramanian A. Effect of fiber diameter on the spreading, proliferation and differentiation of chondrocytes on electrospun chitosan matrices. Cells Tissues Organs 2012;195:207–21.
[27] Shafiee A, Soleimani M, Chamheidari G, Seyedjafari E, Dodel M, Atashi A, et al. Electrospun nano-fiber based regeneration of cartilage enhanced by mesenchymal stem cells. J Biomed Mater Res A 2011;99:467–78.
[28] Chen M, Patra PK, Lovett ML, Kaplan DL, Bhowmick S. Role of electrospun fibre diameter and corresponding specific surface area (SSA) on cell attachment. J Tissue Eng Regen Med 2009;3:269–79.
[29] Nam J, Johnson J, Lannutti JJ, Agarwal S. Modulation of embryonic mesenchymal progenitor cell differentiation via control over pure mechanical modulus in electrospun nanofibers. Acta Biomater 2011;7:1516–24.
[30] Burdick JA, Prestwich GD. Hyaluronic acid hydrogels for biomedical applications. Adv Mater 2011;23:H41–56.
[31] Kim IL, Mauck RL, Burdick JA. Hydrogel design for cartilage tissue engineering: a case study with hyaluronic acid. Biomaterials 2011;32:8771–82.
[32] DeLise A, Fischer L, Tuan RS. Cellular interactions and signaling in cartilage development. Osteoarthritis Cartilage 2000;8:309–34.
[33] Chung C, Burdick JA. Influence of three-dimensional hyaluronic acid microenvironments on mesenchymal stem cell chondrogenesis. Tissue Eng Part A 2009;15:243–54.
[34] Burdick JA, Chung C, Jia XQ, Randolph MA, Langer R. Controlled degradation and mechanical behavior of photopolymerized hyaluronic acid networks. Biomacromolecules 2005;6:386–91.
[35] Sundararaghavan HG, Burdick JA. Gradients with depth in electrospun fibrous scaffolds for directed cell behavior. Biomacromolecules 2011;12:2344–50.
[36] Sundararaghavan HG, Metter RB, Burdick JA. Electrospun fibrous scaffolds with multiscale and photopatterned porosity. Macromol Biosci 2010;10:265–70.
[37] Marklein RA, Burdick JA. Spatially controlled hydrogel mechanics to modulate stem cell interactions. Soft Matter 2009;6:136–43.
[38] Tan E, Lim C. Physical properties of a single polymeric nanofiber. Appl Phys Lett 2004;84:1603–5.
[39] Bian L, Zhai DY, Tous E, Rai R, Mauck RL, Burdick JA. Enhanced MSC chondrogenesis following delivery of TGF-beta 3 from alginate microspheres within hyaluronic acid hydrogels in vitro and in vivo. Biomaterials 2011;32:6425–34.
[40] Legant WR, Miller JS, Blakely BL, Cohen DM, Genin GM, Chen CS. Measurement of mechanical tractions exerted by cells in three-dimensional matrices. Nat Methods 2010;7:969–71.
[41] Schuh E, Hofmann S, Stok K, Notbohm H, Müller R, Rotter N. Chondrocyte redifferentiation in 3D: the effect of adhesion site density and substrate elasticity. J Biomed Mater Res A 2012;100:38–47.
[42] Brenner EK, Schiffman JD, Thompson EA, Toth LJ, Schauer CL. Electrospinning of hyaluronic acid nanofibers from aqueous ammonium solutions. Carbohyd Polym 2012;87:926–9.
[43] Lee K, Jeong L, Kang Y, Lee S. Electrospinning of polysaccharides for regenerative medicine. Adv Drug Deliv Rev 2009;61:1020–32.
[44] Um IC, Fang D, Hsiao BS, Okamoto A, Chu B. Electro-spinning and electro-blowing of hyaluronic acid. Biomacromolecules 2004;5:1428–36.
[45] Carlisle CR, Coulais C, Guthold M. The mechanical stress–strain properties of single electrospun collagen type I nanofibers. Acta Biomater 2010;6:2997–3003.
[46] Gu S, Wu Q, Ren J, Vancso G. Mechanical properties of a single electrospun fiber and its structures. Macromol Rapid Comm 2005;26:716–20.
[47] Yang L, Fitie CFC, van der Werf KO, Bennink ML, Dijkstra PJ, Feijen J. Mechanical properties of single electrospun collagen type I fibers. Biomaterials 2008;29:955–62.
[48] Croisier F, Duwez A-S, Jérôme C, Léonard A, van der Werf KO, Dijkstra PJ, et al. Mechanical testing of electrospun PCL fibers. Acta Biomater 2012;8:218–24.
[49] Biggs M, Richards R, McFarlane S, Wilkinson C, Oreffo R, Dalby M. Adhesion formation of primary human osteoblasts and the functional response of mesenchymal stem cells to 330nm deep microgrooves. J R Soc Interface 2008;5:1231–42.
[50] Biggs M, Richards R, Gadegaard N, McMurray R, Affrossman S, Wilkinson C, et al. Interactions with nanoscale topography: adhesion quantification and signal transduction in cells of osteogenic and multipotent lineage. J Biomed Mater Res A 2009;91:195–208.
[51] Yim E, Pang S, Leong K. Synthetic nanostructures inducing differentiation of human mesenchymal stem cells into neuronal lineage. Exp Cell Res 2007;313:1820–9.
[52] Huang S, Chen CS, Ingber DE. Control of cyclin D1, p27Kip1, and cell cycle progression in human capillary endothelial cells by cell shape and cytoskeletal tension. Mol Biol Cell 1998.
[53] McBeath R, Pirone DM, Nelson CM, Bhadriraju K, Chen CS. Cell shape, cytoskeletal tension, and RhoA regulate stem cell lineage commitment. Dev Cell 2004;6:483–95.
[54] Legant WR, Choi C, Miller JS, Shao L, Gao L, Betzig E, et al. Multidimensional traction force microscopy reveals out-of-plane rotational moments about focal adhesions. Proc Natl Acad Sci 2013;110:881–6.

Please cite this article in press as: Kim IL, et al., Fibrous hyaluronic acid hydrogels that direct MSC chondrogenesis through mechanical and adhesive cues, Biomaterials (2013), http://dx.doi.org/10.1016/j.biomaterials.2013.04.004